

Measurement of the dynamic Young's modulus of porous titanium and Ti6Al4V

Ke Zhu · Chengfeng Li · Zhengang Zhu ·
C. S. Liu

Received: 14 June 2006 / Accepted: 16 January 2007 / Published online: 15 May 2007
© Springer Science+Business Media, LLC 2007

Abstract The dynamic Young's modulus of porous titanium and Ti6Al4V with various porosities was measured using the electromagnetic acoustic resonance method. The dependence of Young's modulus (E) on the porosity (P) has been analysed in detail based on Phani–Niyogi relation $\left(E = E_0 \left(1 - \frac{P}{P_C}\right)^n\right)$ and Pabst–Gregorová relation $\left(E = E_0(1 - aP) \left(1 - \frac{P}{P_C}\right)\right)$. We find that both Phani–Niyogi relation and Pabst–Gregorová relation with fixed material constant $n = 2$ or $a = 1$ but varying P_C can correctly account for the dependence of Young's modulus on the porosity for porous titanium and Ti6Al4V.

Introduction

Titanium and Ti6Al4V are widely used as materials for oral, maxillofacial, and orthopedic implants because of their advantageous mechanical properties and biocompatibility [1–6]. However, a major concern in the practical applications of metallic implant materials in orthopedic surgery is the drastic mismatch of Young's modulus between the bone (10–30 GPa) and the metallic implants (about 105 and 110 GPa for Titanium and Ti6Al4V, respectively). One way to alleviate this problem is to reduce Young's modulus of metallic materials by introducing pores, thereby minimizing damages to tissue adjacent to the implant and eventually prolong device life time [6].

Hence it is important to find the relationship between the porosity and Young's modulus for porous materials. A general expression of the Young's modulus as a function of porosity for the porous medium is of the following form:

$$E = E_0 f(P), \quad (1)$$

where E is the Young's modulus of the porous material and E_0 the Young's modulus of the fully dense material, P is the porosity, $f(P)$ is a function that correlates the Young's modulus to the porosity and is usually obtained fitting the experimental data.

Several semi-empirical and analytical expressions can be found in Refs. [7–10]. Knudsen and Spriggs [7, 8] proposed the following relation:

$$E = E_0 e^{-bP}, \quad (2)$$

where b is a material constant and related to particles stacking. This expression has been widely used to predict the Young's modulus of porous materials with low P , but it is unable to satisfy the boundary condition that E equals zero for $P = 1$. Phani and Niyogi proposed another expression for the Young's modulus [9]:

$$E = E_0 \left(1 - \frac{P}{P_C}\right)^n. \quad (3)$$

where P_C is the critical porosity at which $E = 0$, i.e., the material loses integrity. P_C depends on the stacking geometry of particles, and the material constant n also depends on pore distribution geometry, such as shape, connectivity, etc. Equation 3 satisfies quite well the exact theoretical solution of Young's modulus at various porosities for some model systems with ideal and non-ideal packing geometry. Recently, Pabst and Gregorová

K. Zhu · C. Li · Z. Zhu · C. S. Liu (✉)
Key Laboratory of Materials Physics, Institute of Solid State
Physics, Chinese Academy of Sciences, P.O. Box 1129,
Hefei 230031, P.R. China
e-mail: csliu@issp.ac.cn

have presented a much simple relation [10] which can be written as

$$E = E_0(1 - aP) \left(1 - \frac{P}{P_C}\right), \quad (4)$$

where a is defined as the packing geometry factor. In the case of spherical pore, a is 1, so Eq. 4 can be rewritten as the extremely simple form [10]:

$$E = E_0(1 - P) \left(1 - \frac{P}{P_C}\right). \quad (5)$$

When $P_C = 1$, Eq. 5 reduces to Coble-Kingery relation [10]. Thus Pabst and Gregorová relation can be seen as the general form of the Coble-Kingery relation.

The present paper reports the measurement of dynamic Young's modulus of porous compacts of titanium and Ti6Al4V using an electromagnetic acoustic resonance method. The aim of our study is to test the above-mentioned relation between Young's modulus and the porosity and to verify the available models in light of the experimental data.

Theory of dynamic Young's modulus measurement

In the electromagnetic acoustic resonance method, the sample is excited to flexural vibrations by the Lorentz force from the alternating signals [11]. There will be resonance frequency spectroscopy while varying excited signals. If hanging the sample on the nodal points at the distance from the free end of $0.224l$ and $0.776l$ where l is the whole length, the fundamental resonance mode was measured with the frequency named f_r [12]. On the basis of the motion of flexural vibration, the dynamic Young's modulus, E , is calculated as the following [13]:

$$E = 0.9464 \times 10^{-6} \left(\frac{l}{h}\right)^3 \frac{m}{b} f_r T, \quad (6)$$

where h , b and m is the thickness, width and mass of the sample, respectively. In Eq. 6, T is a correction factor and taken as 1 in the present work.

Experiment procedure

The specimens were prepared by the power metallurgy method which consists of mixing, pressing, and heat-treating steps [4, 5]. Pores were generated after the fugitive space-holders as the second phase were removed during the heat treatment. Commercial pure Titanium and Ti6Al4V

powders (–300 mesh, purity > 98.6%) were used. Urea powders (analytical pure) of –80 + 100 and –60 + 80 mesh were selected as space-holders for titanium and Ti6Al4V, respectively. Metal powders and urea powders were well mixed in an agate mortar, then the mixtures were compacted in a stainless-steel die with 250 MPa pressure, resulting in a semifinished product in which urea powders were distributed homogeneously. Porous metals were then obtained by heating the semifinished material at 200 °C for 2 h to burn out urea powders. In order to increase their mechanical strength, the obtained porous metals were given a sintering treatment at 1200 °C for 2 h. By changing the weight ratio of metal powders to urea powders, samples with various porosities ranging from 30% to 66% were prepared. The size of all samples was cut to $2 \times 4 \times 60$ mm by an electrosparking machine. The porosity of each specimen was calculated from measurements of its weight and apparent volume. Microstructures of the porous titanium and Ti6Al4V samples were observed with a scanning electron microscope (SEM) and displayed in Fig. 1.

Results and discussions

Figures 2a and b show the plots of the relative Young's modulus versus the porosity of titanium and Ti6Al4V, respectively, along with the curve fits obtained using Eqs. 2–4. A glance of Figs. 2a, b shows that Young's modulus decreases with increasing porosity and, both Eqs. 3 and 4 provide a satisfactory fit for the porosity dependence of relative Young's modulus, but Eq. 2 gives a poor description of the porosity dependence of relative Young's modulus. It should be noted that Eqs. 3 and 4 involve two adjustable parameters while Eq. 2 only involves one adjustable parameter. The curve fits obtained with Eqs. 2–4 yield the values of these adjustable parameters, which are presented in Table 1.

As can be seen from Table 1, the obtained value of P_C of porous Ti6Al4V is a bit higher than that of porous titanium, suggesting that the space-holders particle size has effect on P_C . In other words, the space-holders particle size is larger, the value of P_C is higher. The effect of the space holders on P_C can be explained with the porosity model based on minimum solid area of particles or bubbles stacking [9, 18]. In our porous metallic materials, pores are fabricated by burning out space-holders. The particles stacking geometry will vary with the ratio of the space-holder particle size to the metal particle size. When the space-holder particle size is far larger than that of metal particle, the pore structures can be considered as bubbles stacking, the value of P_C is close to 1; whereas the space-holder particle size is far smaller than that of metal particle,

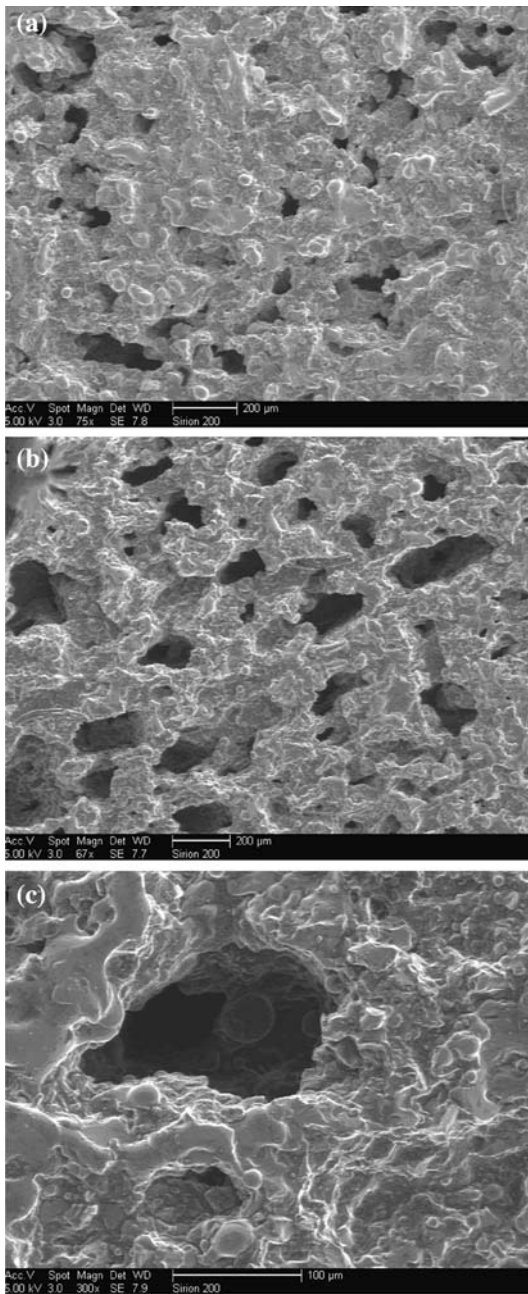


Fig. 1 SEM micrographs of porous titanium and Ti6Al4V. (a) porous titanium (the average pore size 170 μm), (b) porous Ti6Al4V (the average pore size 220 μm), (c) micrograph of one pore

the pore structures can be considered as particles stacking, the value of P_C is below 0.476 [18, 20]. Thus, it may be expected that the value of P_C increases with the increase in the ratio of space-holder particle size to metal particle size. In our present experiment, the ratio of space-holder particle size to Ti6Al4V metal size is about 8:1, which is larger than that of the space-holder particle size to titanium metal size with 6:1. As a result, the value of P_C of porous Ti6Al4V is a little higher than that of porous titanium.

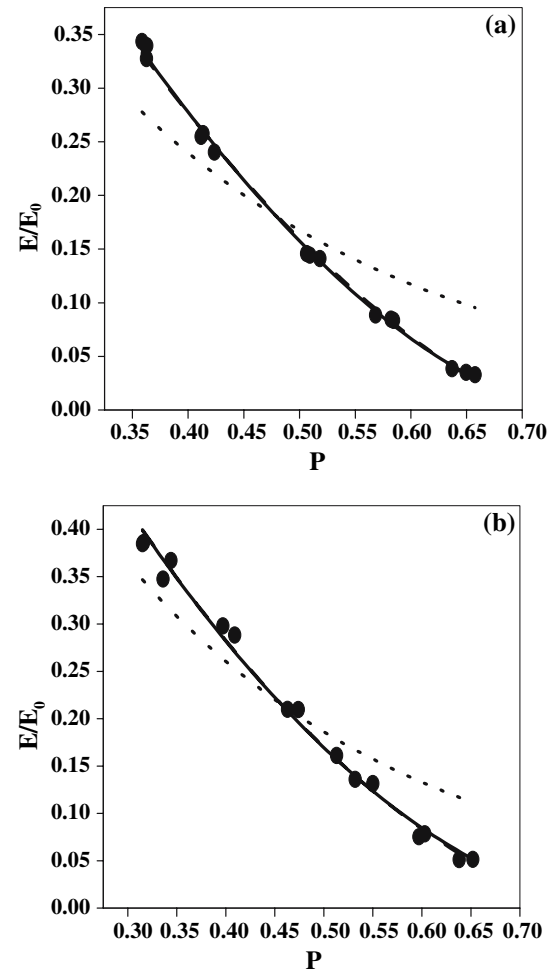


Fig. 2 Young's modulus is plotted against the porosity of porous titanium (a) and Ti6Al4V (b), along with the curve fits obtained using Knudsen–Spriggs relation (Eq. 2, the *dotted line*), Phani–Niyogi relation (Eq. 3, the *solid line*) and Pabst–Gregorová relation (Eq. 4, the *dash line*)

The material constant n of Phani–Niyogi relation is related to pore geometry, such as pore shape, connectivity, etc [9]. The material constant a in Pabst–Gregorová relation is also related to pore shape. From Table 1, it can be seen that the value of $n \approx 2$ and $a \approx 1$, respectively. According to the conclusions by Phani [9, 14] and Pabst [10], the present results of $n \approx 2$ and $a \approx 1$ indicate that pores in our porous metallic materials are approximately spherical.

Because both Phani–Niyogi relation and Pabst–Gregorová relation agree with the experimental data, there may exist a certain correlation or link between them. In order to find their link, we expand Eq. 3 in a power series of P :

$$E = E_0 \left(1 - \frac{n}{P_C} P + \frac{n(n-1)}{2P_C^2} P^2 - \frac{n(n-1)(n-2)}{6P_C^3} P^3 + \dots \right). \quad (7)$$

Table 1 The adjustable parameters in Eqs. 2, 3 and 4 obtained the best fits to the experimental data of Young’s modulus-porosity for porous titanium and Ti6Al4V

Materials	Porosity range (%)	Eq. 2	Eq. 3		Eq. 4	
		<i>b</i>	P_C	<i>n</i>	<i>A</i>	P_C
Titanium	35–66	3.57 ± 0.15	0.75 ± 0.01	1.68 ± 0.04	0.89 ± 0.039	0.70 ± 0.01
Ti6Al4V	30–66	3.36 ± 0.12	0.83 ± 0.03	1.93 ± 0.11	1.01 ± 0.09	0.76 ± 0.04

Equation 4 can be rewritten in powers of *P* as the following form:

$$E = E_0 \left[1 - \left(a + \frac{1}{P_C} \right) P + \frac{a}{P_C} P^2 \right]. \tag{8}$$

The coefficients of the first-, second- and third-order terms in Eq. 7 and the coefficients of the first- and second-order terms in Eq. 8 have been calculated using the data presented in Table 1. These coefficients are summarized in Table 2. As can be seen from Table 2, for porous titanium it is 0.06 (i.e., 3% increases or decreases in the magnitude) that the difference in the coefficients of the first-order term between Eqs. 7 and 8, whereas for porous Ti6Al4V almost no difference between the first-order-term coefficients. Similarly, for porous titanium it is 0.25 (13%) that the difference in the second-order-term coefficients, but for porous Ti6Al4V it reduces to 0.03 (2%). For porous titanium the coefficient of the third-order terms in Eq. 7 is 0.15, but for porous Ti6Al4V it is 0.03 and could be neglected. We believe that, for porous Ti6Al4V it is a negligible third-order term in Eq. 8 that results in the tiny differences in the coefficients of the first- and second-order terms between Eqs. 7 and 8. Thus, Phani–Niyogi relation should reduce to Pabst–Gregorová relation for the dependence of Young’s modulus on porosity when the third-order term in Eq. 8 is negligible.

During the above-mentioned processes of fitting Eqs. 3 and 4 to the porosity dependence of Young’s modulus, we find that the fits are very good but the adjustable parameters (P_C , *n* and *a*) in Eqs. 3 and 4 show the dependence upon the selected porosity ranges, which are shown in Table 3. For example, for porous titanium with porosities 40–66% the obtained P_C and *n* in Eq. 3 are 0.77 and 1.76, respectively, whereas in the porosity range 35–58% P_C and *n* are

adjusted to be 0.73 and 1.60. Compared to porous titanium, the dependence of both P_C and *n* on the selected porosity ranges is stronger in porous Ti6Al4V: in the porosity range 35–66% the obtained P_C and *n* in Eq. 3 are 0.77 and 1.66, respectively, whereas in the porosity range 30–55% P_C and *n* are adjusted to be 0.93 and 2.24, respectively. Similar results have been reported by Kováčik [15] in the analysis of the experiment data of sintered iron. No doubt this is the bad effect on Eqs. 3 and 4 with two adjustable parameters (*n* and P_C or *a* and P_C) and limits their applicability. Reducing two adjustable parameters to only one may greatly weaken this unfavorable effect.

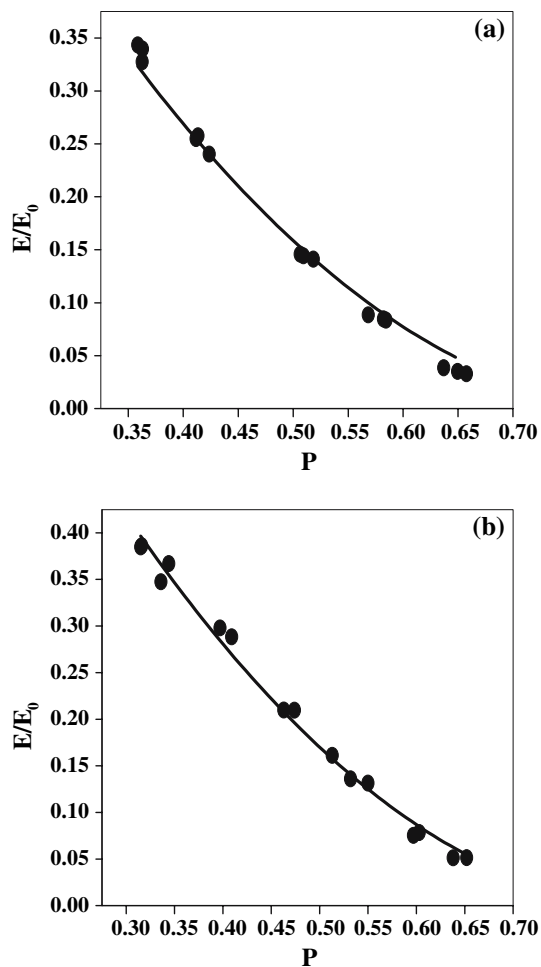
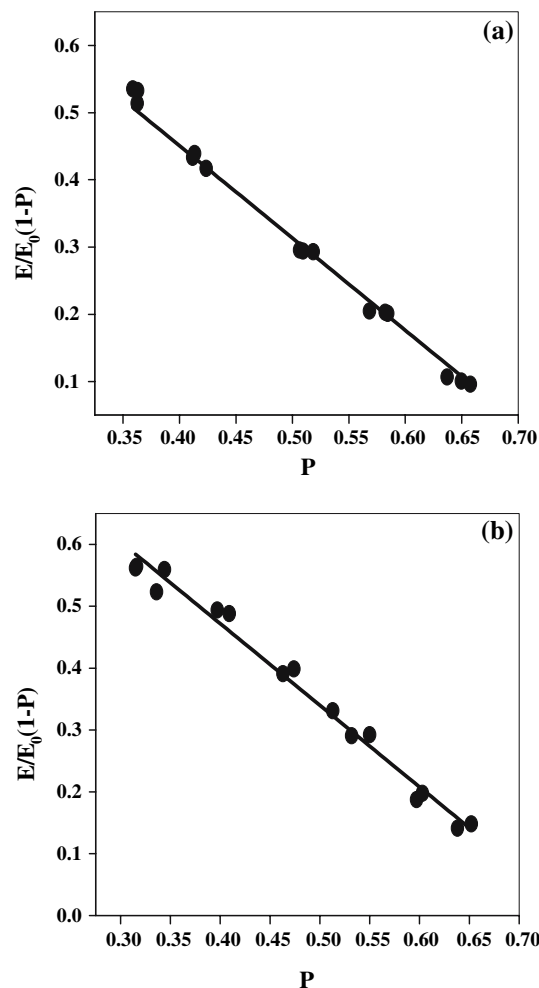
Rice has ever proposed a minimum solid area (MSA) method [16–20] to determine P_C . However, for most real porous materials the value of P_C cannot be determined exactly except for those with idealized stacking of spherical particles. Kováčik, Matikas, Coronel and co-workers [15, 21, 22] used the tap porosity as P_C in Eq. 3 to fit sintered α_2 titanium aluminide and sintered glass. They found that the experimental results can be fitted rather well in low-porosity region but badly in high-porosity region. In addition, they also used the initial powder porosity as P_C and found it can give satisfactory fit only for sintered glass. Thus, the value of P_C should be determined from fitting the experimental data. In other words, P_C should be an adjustable parameter. Another way is to let P_C as an adjustable parameter and fix the exponent *n* or the parameter *a*. When pores are modeled simply by spherical bubbles for porous titanium and Ti6Al4V, the exponent *n* equals to 2 in Eq. 3 and, the parameter *a* equals to 1 in Eq. 4. Using *n* = 2 and *a* = 1 we have fitted Eq. 3 (i.e., Phani–Niyogi relation) and Eq. 4 (i.e., Pabst–Gregorová relation) to the porosity dependence of Young’s modulus as shown in Figs. 3 and 4, respectively. From Figs. 3 and 4, it can be seen that both Phani–Niyogi relation with *n* = 2 and

Table 2 The coefficients of the first-, second- and third-order terms in Eq. 7 plus the coefficients of the first- and second-order terms in Eq. 8 calculated using the data presented in Table 1

Materials	Coefficients				
	Eq. 7			Eq. 8	
	1st-order term	2nd-order term	3rd-order term	1st-order term	2nd-order term
Titanium	–2.26	1.02	0.15	–2.32	1.27
Ti6Al4V	–2.33	1.30	0.03	–2.33	1.33

Table 3 The two adjustable parameters P_C , n or a in Eqs. 3 and 4 obtained from the best fits of the experimental results for porous titanium and Ti6Al4V over different porosity ranges

Materials	Porosity range (%)	Eq. 3		Eq. 4	
		P_C	n	a	P_C
Titanium	40–66	0.77 ± 0.01	1.76 ± 0.03	0.97 ± 0.02	0.72 ± 0.01
	35–58	0.73 ± 0.02	1.60 ± 0.06	0.78 ± 0.06	0.67 ± 0.01
Ti6Al4V	35–66	0.77 ± 0.01	1.66 ± 0.05	0.85 ± 0.05	0.72 ± 0.01
	30–55	0.93 ± 0.08	2.24 ± 0.26	0.96 ± 0.23	0.76 ± 0.19

**Fig. 3** Young's modulus is plotted against porosity for porous titanium (a) and Ti6Al4V (b). The *solid lines* are curve fits obtained using Phani–Niyogi relation with fixed $n = 2$ **Fig. 4** Young's modulus is plotted against porosity for porous titanium (a) and Ti6Al4V (b). The *solid lines* are curve fits obtained using Pabst–Gregorová relation with fixed $a = 1$

Pabst–Gregorová relation with $a = 1$ can correctly account for the porosity dependence of Young's modulus over the entire porosity. Table 4 lists the adjustable parameter P_C obtained by the fitting with Phani–Niyogi relation and Pabst–Gregorová relation at various porosity ranges. In sharp contrast to the results presented in Table 3, the only adjustable parameter P_C is nearly independent of the

selected porosity range, suggesting that the influence of irregularity of pore shape on the Young's modulus-porosity relation may be negligible. Thus, we may conclude that, both Phani–Niyogi relation and Pabst–Gregorová relation with the only adjustable parameter P_C are applicable to the dependence of Young's modulus on porosity for porous materials.

Table 4 The only adjustable parameter P_c in Eqs. 3 and 4 with $n = 2$ or $a = 1$ obtained from the best fits of the experimental results for porous titanium and Ti6Al4V over different porosity ranges

Materials	Porosity range (%)	Eq. 3 ($n = 2$) P_c	Eq. 4 ($a = 1$) P_c
Titanium	35–66	0.831 ± 0.005	0.728 ± 0.004
	40–66	0.832 ± 0.004	0.724 ± 0.002
	35–58	0.835 ± 0.005	0.731 ± 0.006
Ti6Al4V	30–66	0.851 ± 0.005	0.757 ± 0.006
	35–66	0.856 ± 0.006	0.761 ± 0.006
	30–55	0.856 ± 0.006	0.763 ± 0.008

Conclusions

We have preformed the measurement of the dynamic Young’s modulus of porous titanium and Ti6Al4V with various porosities by the electromagnetic acoustic resonance technique. We fit Phani–Niyogi relation and Pabst–Gregorová relation with two adjustable parameters to the porosity dependence of Young’s modulus for porous titanium and Ti6Al4V over a wide range of porosity. Although these two relations work well for the porosity dependence of Young’s modulus, the adjustable parameters (P_c , n or a) show the dependence on the selected porosity ranges, which limits their applicability. If using $n = 2$ and $a = 1$, these two relations also correctly account for the porosity dependence of Young’s modulus and the left adjustable parameter P_c is nearly independent of the selected porosity ranges. Thus, we may conclude that both Phani–Niyogi relation and Pabst–Gregorová relation with the only adjustable parameter P_c and with fixed values of $n = 2$ or $a = 1$ are applicable to the dependence of Young’s modulus on porosity for porous materials.

Acknowledgments This work was supported by the Natural Science Foundation of China under grant Nos. 10374089 and 10674135 and the Knowledge Innovation Program of Chinese Academy of Sciences under Grant No KJCX2-SW-W17.

References

1. Kutty MG, Bhaduri S, Bhaduri SB (2004) J Mater Sci: Mater Med 15:145
2. Li JP, Li SH, Van Blitterswijk CA, De Groot K (2006) J Mater Sci: Mater Med 17:179
3. Oh I, Nomura N, Masahahi N, Hanada S (2003) Scripta Mater 49:1197
4. Dunand DC (2004) Adv Eng Mater 6:369
5. Wen CE, Yamada Y, Shimojima K, Chino Y, Hosokawa H, Mabuchi M (2002) J Mater Res 17:2633
6. Li CF, Zhu ZG (2006) J Porous Mater 13:21
7. Knudsen FP (1959) J Am Ceram Soc 44:376
8. Spriggs RM (1961) J Am Ceram Soc 44:628
9. Phani KK, Niyogi SK (1987) J Mater Sci 22:257
10. Pabst W, Gregorová E (2004) J Mater Sci 39:3501
11. Nowich S, Berry BS (1972) Anelastic relaxation in crystalline solids. Academic Press, New York; London, p 626
12. Wolfenden A, Harmouche MR, Blessing GV, Chen YT, Terranova P, Dayal V, Kinra VK, Lemmens JW, Phillips RR, Smith JS, Mahmoodi P, Wann RJ (1989) J Test Eval 17:2
13. Spinner S, Tefft WE (1991) Proc ASTM 61:1221.K
14. Phani K, Mukerjee RN (1987) J Mater Sci 22:3453
15. Kováčik J (1999) J Mater Sci 18:1007
16. Rice RW (1993) J Am Ceram Soc 76:1801
17. Rice RW (1996) Key Eng Mater 115:1
18. Rice RW (1996) J Mater Sci 31:102
19. Rice RW (1996) J Mater Sci 31:1509
20. Rice RW (2005) J Mater Sci 40:983
21. Matikas TE, Karpur P, Shamasundar S (1997) J Mater Sci 32:1099
22. Coronel L, Jernot JP, Osterstock F (1990) J Mater Sci 25:4866